METALLURGICAL CONSIDERATIONS ON CRACK PROPAGATION

E.R. de los Ríos
Department of Mechanical Engineering, University of Sheffield, Mappin Street, Sheffield, U.K.

The effect of metallurgical variables on crack propagation can best be appreciated by first looking at the various stages of fatigue crack growth (Fig. 1).

The first stages in the growth of a fatigue crack are highly dependent on the microstructure of the material. Cracks are initiated either by extrinsic surface defects such as machine marks, pores, voids, etc, or by extrinsic defects such as intrusions or extrusions and grain boundaries. The initiated crack continues to grow in stage I by a shear mechanism along the persistent slip band (psb). This is the microstructural stage of short crack growth (MSC) showing that periods of high growth are followed by periods of low growth. This period may extend for two or three grains (d_1, d_2, d_3). The crack may also halt several times at microstuctural barriers then continue to propagate before it enters a period of more steady growth which is the physical small crack period.

This zone is bounded by the MSC at small crack lengths and by the LEFM zone at longer crack lengths. The boundary with the MSC region depends on the length of the dominant microstructural barrier which depend on stress level and microstructural features. The boundary with the LEFM zone is both stress and crack lengths dependent and is related to the transition point between the structure-sensitive mode of crack growth towards the threshold branch of the long crack growth rate curve and the structure-intensitive mode in the upper branch. This transition point has been examined by various authors, for example, Taylor quotes $l_2 = 10d$ (crack length equal to ten times the grain diameter), Yoder et al states that the transition takes place when the reversed plastic zone size is of the order of the grain size. It follows that $K_T = 5.5\ \sigma_{ys}\ \sqrt{d}$, and also Liu and Liu, determined an empirical expression for this transition as $K_{th} = (0.7 \pm 0.1)\ K_t$.

The boundaries between these different types of crack regimes can also be established by using modified Kitagawa-Takahashi diagrams. A particularly useful map of this kind is that developed by Brown in which six different fatigue fracture mode zones are easily distinguished. In here the LEFM region is limited to below stress range of $2\sigma_{cy}/3$ (where σ_{cy} is the cyclic yield stress) to comply with small scale yielding (SSY) conditions. At higher stress range levels up to a limit of $2\sigma_T$ (where σ_T is the tensile strength) cracks are described by EPFM analysis, growing by either a mode I or a mode III mechanism according to stress levels. In the microstructural crack region crack growth is by stage I but at low stress levels, the limited plasticity at the tip of the crack can be accommodated by slip in first one slip system and consequently the mode of fracture is crystallographic. Cracks can form at stresses below the fatigue limit as long as platicity, even in the most elementary form, can be activated, so that the limit for crack initiation should theoretically be as low as the stress required for psb formation. Fig. 2.

Short crack propagation

Before discussing the methods used to study short crack growth a description of the experimental technique used in the formation and monitoring of short cracks will be briefly given.

Techniques used to initiate short crack growth

The most common forms of fatigue loading used in the study of short cracks are axial, bending and torsion. In particular, the latter, using hour-glass specimens proved to be a very useful combination for the following reasons (see Fig. 3).

i) the surface area for crack initiation is restricted to the central portion of the specimen without unduly introducing stress concentrations.

ii) in torsional loading, because cracks grow preferentially along the surface, cracks remain in stage I for longer time (length) so that this important stage of crack growth can be studied much more thoroughly.

Techniques used to monitor short crack growth

Possibly the most popular method used at present to detect and monitor short fatigue cracks is the replication method. Its popularity stems from its simplicity, reproducibility, quickness (the test has to be stopped for only a few minutes) and the facility of storing the replicas in a library type system for future reference.

In essence, the method consists of taking replicas at given intervals over the test period and then observing them in the reverse order, commencing with the latest replica where the main cracks can be easily located, and working backwards through the series. If the surface of the specimen is etched, then there will be a large number of reference points for helping in the location of the same crack or area whilst examining the next replica. If the specimens is unetched, or there are a few reference points, then it may be necessary to inscribe marks on the specimen surface away from the most likely fatigue crack initiation area (i.e. micro-hardness indentation marks a few a millimeters away from the minimal cross-section area in an hour-glass shape specimen). These reference marks are used as the origin of a co-ordinate system to build-up a map with the location of all features of interest (i.e. cracks). The series of replicas constitutes, therefore, a chronological record of the whole fatigue damage process.

On completion of the test, the series of replicas is examined to yield quantitative data which can be used to derive empirical expressions for crack growth, life prediction exercises, or to test theories or models for short crack growth propagation. The most pertinent data related to crack growth experiments is crack length and crack orientations. The former is used to obtain crack growth rate and the latter the direction of crack growth.

These operations can be easily performed with the aid of image analysis equipment, which should allow the operator to

i) define the origin and orientation of the co-ordinate system to which position and orientation of cracks will be related.

ii) keep several images in the frame store at any one time.

iii) calibrate the system according to the magnification used and to commpensate for distortions that may exist in the microscope lens or camera.

iv) be able to cope with cracks extending by more than one frame length.

Accoustic Microscopy

Although direct observation of fatigue specimens or the examination of replicas buy optical microscopy is extensively used in fatigue short crack research and valuable information has and will still continue to be obtained, there are some practical limitations inherent in these methods which are extremely difficult to overcome. Firstly is the problem of limited resolution - between 0.5- 1μm for an optical microscope, which coupled with the difficulty of finding replicating material to duplicate very fine details, means that very fine cracks will pass unnoticed when using these methods. Secondly, is the masking effect of other features on the specimen surface which hides the presence of the crack. the typical case is low and medium carbon steel specimens where the first sign of fatigue damage is the formation of multiple persistent slip bands (psb) which form and extend across ferrite grains. A small proportion of these psb contain cracks which initially grow along the psb plane. Within this stage of growth the cracks are indistinguishable from the psb until at a much later stage, the crack begins to propagate into the adjacent grain, see Fig. 4. Scanning acoustic microscopy (SAM) offers the possibility of overcoming this limitation without any need for replicas. In a SAM, the contrast arises from the interaction of the sound beam with the elastic properties of the material.

The basic components and operations of the SAM can be described with the help of Figure 5. A piezoelectric transducer converts the transmitted radio frequency (RF) electromagnetic pulses to acoustic pulses which are brought to a focus at the focal plane of the lens. Pulses reflected from the object are collected by the same lens, and the transducer converts them back to electrical pulses which, after detection, provide a video signal. This signal is the input to the display system and is used to intensity-

modulate an electron beam on the display monitor. Conversely, this signal is passed onto a frame store which holds that value for intensity at an address that corresponds to the position of the lens, relative to the specimen. The lens is scanned over the field of view, in a raster manner, in synchronism with the electron beam on the display, or conversely its position is measured (for example by a transducer) and then fed to the frame store. The image is thus built up point by point.

In acoustic microscopy the two important waves considered in the interpretation of images are the normal to the surface of the specimen and the incident on the specimens at the Rayleigh angle, Fig. 6. The best contrast is attained when the specimen is marginally defocussed towards the lens (-z) because this enhances the interference between the normal and Rayleigh reflections. The image then becomes sensitive to anything that affects the propagation of Rayleigh waves.

The special case considered here is that of surface cracks and, in particular, fine and close cracks or cracks which are masked by other features such as deformation bands. Incident waves that are geometrically reflected from the surface will be negligibly affected by the crack, in light microscopy in particular, a crack that is finer than the resolution will not normally be detectable. Rayleigh waves would, on the other hand, strike the cracks from the side and therefore would be strongly affected by cracks of even less than a wavelength.

In Fig.7 a SAM and a optical image taken at the same location within the cross-section of a 316 stainless steel fatigue specimen with some very fine surface cracks are compared. One particularly fine crack is almost undetectable with the optical microscope, Fig. 7a, even the first short segment being scarcely visible. The acoustic micrograph, Fig. 7b, some of the grain contrast.

In conclusion, it will be seen from the evidence now presented, that a scanning and fatigue system can be designed in such a way that a given test can be continuously monitored to study the formation of cracks and short crack propagation, in-situ, during the progress of the fatigue test. It will be possible, without etching, to measure the length of cracks, or microstructural features, estimate their orientation, and establish their relationship to grain structure and second phases.

Microstructural short cracks

Irrespective of the precise cause (inclusions, micronotches, etc) by which fatigue cracks are initiated, they propagate along slip bands, Figure 4 which illustrates this situation clearly, shows the various stages in the development of a crack. In Fig. 4(b) slip bands are seen to form preferentially along the applied maximum shear directions but not all the grains with a favourably orientated slip system will be able to generate slip bands. Plastic deformation is facilitated in b.c.c. metals because of the multiplicity of slip systems available; in iron the {101}, {211} and {123} all act as slip plane with the direction of slip always being the close-packed direction [111] which is common to all three sets of planes. At a later stage [Fig. 4 (c)] a crack is seen to have grown along the slip band and extends through its entire length. The crack as yet as not been able to break through the ferrite grain boundaries at either end and consequently there is a temporary of crack growth. The reason why the crack has not been able to propagate into the adjacent grain is undoubtedly due to the difference in orientation of the two grains. One grain is orientated to permit slip along the maximum shear direction parallel to the specimen axis while the other grain is placed to slip along the complementary maximum shear direction transverse to the specimen axis. Nevertheless, these crystallographic barriers to crack propagation are not impenetrable and the crack continues to grow once this partial barrier has been in the second grain.

Barriers of a more formidable nature to crack progation are the pearlite regions where many of the cracks, particularly transverse cracks may be arrested.

This example gives a clear indication of the importance of microstructural barriers to crack growth in the development of new fatigue resistance materials. A fine grain size is beneficial in both the microstructural and the physical crack growth region. In the former, by increasing the number of barriers that the short crack has to overcome before entering the next stage of crack growth, and in the latter by increasing the value of the new flow stress in the plastic zone through the well known Hall-Pecth relationship $\sigma_y = \sigma_o + K_y d^{-1/2}$.

A higher flow stress means a smaller plastic zone size, a smaller crack tip plastic displacement and consequently a lower crack growth rate.

The example also shows the effect of anisotropy on crack growth rate. If the material shows a preferred crystallographic orientation there would be no change in crack growth direction on crossing a grain boundary. In terms of the strength of barriers they will be weak barriers and the retardation in crack growth rate will be minimal.

The other aspect illustrated by the example is relative resistance of the various microstructural constituents to crack propagation. The pearlite, in this case, offers a much larger resistance to crack propagation than the ferrite. This is in relation to their different flow stresses. All the parameters used to characterised crack growth rate such as crack tip opening displacement or plastic zone size are inversely related to the crack tip flow stress of the material and consequently a crack will be retarded or even stopped when its tip comes against a high strength constituent.

The effects of grain size, precipitates and uniaxial microstructures is illustrated in schematic form in Figure 8. Fine grain structures have a lower crack growth rate in the short crack region, due to the smaller crack tip plastic zone, but a larger crack growth rate in the near threshold region. This is due mainly to two reasons, the first being a higher threshold value for fine grain materials, which is related to the higher yield stress and the second to the lower contribution of surface roughness friction.

The effect of precipitates is different according to whether they are shearable by dislocations (under-aged, UA) or not shearable (over-aged, OA). The largest differences between the two extreme types seem to occur in the vicinity of the microstructural barriers to short crack growth slip occurring in the plastic zone at the crack tip is more reversible in under-aged structures. For a crack growing along a single slip band at the crack tip, the crack propagation rate should be proportional to the number of dislocations emitted along the slip plane during the loading half of the cycle which do not return along the same plane during the unloading half. The number of dislocations which contribute to crack advance in each cycle is thus directly related to heterogeneity of the strain, i.e., the ease of cross-slip. The superior near threshold crack propagation resistance of the UA condition is mainly due to the increased slip reversibility although some effect of increased crack deflection cannot be ruled out.

Regarding the microstructural effects of two phase alloys, some evidence suggests that large differences in behaviour can be observed when the second phase is softer as opposed to harder than the primary phase.

The stress intensity factor ahead of the crack is enhanced in the proximity of soft phase while the opposite occurs with a hard phase giving a type of behaviour illustrated by Fig.8c. The initial part of the short crack region should be common to the three alloys showing the usual deceleration of crack growth rate with crack length. The pure ferrite will show just one main dip in the curve, coincident with the tip of the crack approaching the ferrite grain boundary. The other two alloys will show another dip related to the location of the second phase along the crack path. The alloy with the harder second phase will show the largest deceleration. Therefore the steel containing cementite will show the deepest dip.

Short Crack Modelling

Short cracks are not amenable to LEFM characterization for several reasons. The stress required for short crack growth are greater than $\sigma_{cy}/3$, usually quoted as the limit for LEFM; the large plastic zone associated with a short crack invalidates the necessary condition for LEFM crack tip plasticity of small scale yielding (SSY). Miller for example gives the follwing values for the limits of applicability of LEFM; if the plastic zone size $r_p = a/50$ (a: crack length), $\Delta K = \Delta\sigma\sqrt{\pi a}$ and $r_p = A(\Delta K/\sigma_{cy})^2$ with $A = 0.1$, then $\sigma < 0.3\sigma_{cy}$. The limiting crack length was estimated to lie in the range 0.1 to 0.5 mm. Below this range LEFM cannot be applied, because the applied stress to cause crack growth will be too high and the stress strain field at the crack tip will not be quantified with sufficient accuracy.

Elasto-plastic fracture mechanics (EPFM) solutions have to be developed, therefore, to describe short fatigue crack growth rate. The approach for any mode of crack growth should be able to regard the peculiarities of short and long cracks, namely, the accelerating and decelerations arrest at stresses below the fatigue propagation threshold for a given crack length, strength of microstructural barriers, crystal orientations, work hardening transition to long crack behaviour and finally long crack growth.

Two approaches developed here in Sheffield which deal with most of the points raised above related to the behaviour of short cracks will be described next.

The Two Equations Approach

The first is the empirical approach of Hobson who suggest equations of the type

$$\frac{da}{dN} = c\,(d - a) \qquad (1)$$

for the short crack region, and

$$\frac{da}{dN} = Ga - D \qquad (2)$$

for the physical small crack and long crack region. The coefficients C, G and D are obtained through fitting the two equations to experimental data; C and G depend on the applied stress while D is a constant for the material and represents the crack growth threshold. The point of intersection of the regression line with the abscissa in Fig. 9 gives the value of d, which is also of the same order as the distance to the dominant microstructural barrier to fatigue crack growth. When fitting equations of this type to experimental data the values of C and G are stress/strain dependents and a large scatter is observed. Such a dispersion is to be expected due to some cracks being able to propagate much more quickly than others because of variations in the crystallographic orientations of individual grains and also proximity of other cracks.

Assuming that the fast growing cracks are more likely to cause failure a statistical representation of the fastest growing observed cracks should be employed to estimate the stress dependent values of C and G.

For a 0.4 C steel Hobson found that the following expressions fit satisfactorily the data

$$\frac{da}{dN} = 1.64 \times 10^{-34}\,(\Delta\sigma)^{11.14}\,(d-a) \qquad (3)$$

and

$$\frac{da}{dN} = 5.4 \times 10^{-23}\,\Delta\sigma^{6.54}\,a\,4.24 \times 10^{-3} \qquad (4)$$

Fig. 9 shows the range of valid crack lengths for the application of each equation. Region (1) the microstructural crack zone where equation (1) is used to calculate fatigue life in this period. Region (2) is the interactive zone where both the microstructural and fracture mechanics mechanisms, equation (1) and (2) operate and finally in the continuum fracture mechanics region (3), equation (3) is used. By considering the three areas of crack growth the lifetime can be calculated, Table I.

A single equation approach

This model developed by Navarro and De los Rios is based on two fundamental works; one by Bilby et al. about the spread of plasticity at a crack tip, and the second by Petch on the yielding of polycrystal metals. The model considers a crack initiated at the surface by an inclusion or a hard second phase particle or by localized plastic deformation on a psb (intrusions or extrusions). The crack proceeds to grow along the psb which is blocked by the grain boundary and it will remain blocked for as long the stress ahead of the slip band is unable to initiate slip in the next grain. As the crack grows, the stress concentration ahead of the blocked slip band increases, until it attains a value sufficiently high to operate a dislocation source in the next grain. At this point the plastic zone (slip band associated with the crack extension process) extends right across the next grain. This obviously means that the plastic-elastic interface should coincide at every instant with a grain boundary.

If the applied stress is below the fatigue limit, the stress ahead of the slip band will not be suffiently high to initiate slip in the next grain and therefore the crack will arrest on reaching the grain boundary.

Since crack growth rate is proportional to the plastic zone size it will decrease as the crack lengthens, up to the point where slip is initiated in the next grain; the plastic zone size increases suddenly by a length equivalent to the grain size and so does crack growth rate. This intermittent growth rate of the crack will dampen its oscillations, as the crack becomes longer until, at the transition length from microstructurally short to a physically small crack, the oscillations will cease and there will only be a monotonic increase of crack growth rate.

Theory

For the full proof of the equation which follow the reader is directed to the original references listed at the end of the test.

After solving the equilibrium equations for all the internal and external forces acting on the system, the equation for the plastic displacement at the tip of the crack is determined for conditions where the applied

stress σ is much higher than the friction stress as:

$$\phi = \frac{2}{G}\frac{\sqrt{1-n^2}}{n}\sigma a \qquad (5)$$

where ϕ: crack tip plastic displacement
n: a/c
a: half surface crack length (Fig.10)
c: half surface crack length and plastic zone size
σ: applied stress
G: shear modulus

Many models proposed to described crack growth rate in elasto-plastic conditions considered da/dN as a function of crack tip displacement. Following similar argument,

$$\frac{da}{dN} = f\,\phi \qquad (6)$$

A theoretical estimation of the factor f is extremely difficult since knowledge of the dislocation storage and annihilation rate would be required in order to calculate the fraction of dislocations actually involved in crack extension. An empirical determination of this factor, is however, possible if short crack growth rate data from at least three levels of stress is available. As an example using 0.4 C steel it varied from approximately 0.025 to 0.25 over a range of applied stress 630-1000 MPa.

The condition for crack propagation in this model is governed by the stress ahead of the plastic zone being able to operate dislocation sources in the next grain and is given by:

$$\frac{s(\xi o)}{\sigma} = \frac{1}{\sqrt{2}}\frac{1}{\sqrt{\xi o - 1}}\left[1 - \frac{2}{\pi}\frac{\sigma_o}{\sigma}\cos^{-1}n\right] + \frac{\sigma_o}{\sigma} \qquad (7)$$

where ξ^o: $(r_o + c)/c$
r_o: distance from the grain boundary to the nearest dislocation source in the next grain
σ_o: friction stress

For a constant amplitude applied stress and a given friction stress, the stress concentration ahead of the plastic zone depends solely on the parameter n. As the crack grows, but with the plastic zone still being blocked by the grain boundary, the parameter n increases towards a critical value $n = n_c$, at which point, the stress concentration reaches a level sufficiently high to activate dislocation sources and consequently, the plastic zone extends right across the next grain. In the same interval crack growth rate decreases to its lowest value.

Upon slip transmission, the value of n changes suddenly to the new lower value n_s related to the larger plastic zone.

$$n_s = n_c \frac{i}{1+2} \quad \text{for } i = 1,3,5... \qquad (8)$$

where i is the number of half grains transversed by the crack. In response to a lower value of n crack growth rate suddenly increases to a new maximum (equation 5).

The discontinuous character of the slip transfer (slip-jumps) is repeated grain after grain, giving an oscillating pattern to crack growth, Fig.11. It is the relative importance of these jumps upon the overall description of crack growth that differentiates the microstructurally short and the physical short crack period, the latter being described by continuum mechanics.

The stress concentration is at a maximum when $n = 1$ (i.e. when the crack reaches the grain boundary where the plastic zone is blocked); but even at this maximum level, particularly when the applied stress level is low, the stress might still be insufficient to initiate slip in the next grain and, consequently, the crack arrests, i.e. the plastic displacement is zero in equation (5).

The fatigue limit σ_{FL} is therefore identified with the applied stress below which a crack that has grown within one grain ($a = D/2$) is unable to initiate slip in a neighbouring grain. When the non-propagation condition is considered for a crack spanning over an arbitrary i number of half grains ($a = c = iD/2$), the stress equivalent to the fatigue limit for this crack length, σ_{Li}, is related to the actual fatigue limit through the simple relation

$$\sigma_{Li} = \frac{\sigma_{FL}}{\sqrt{i}} \qquad (9)$$

If the number i of half grains transversed by the crack is large then the incremental ratio between the slip jump-length and crack length $\Delta i/i$ ($=2/i$) is small and, therefore, the stress σ_{Li} defined above may be considered to be little affected by the slip jumps and to vary continuously.

Equation (7) is used to determine the value of n_c in every grain by equating $S(\xi o)$ with σ_{Li} and through (9), with σ_{Fl}. Thus, knowing the fatigue limit, estimating the values of the friction stress and assuming that a dislocation source is located at a distance of approximately one micron, equation (7) fixes the values of n_c in each interval of slip.

Once n_c has been determined, n_s is calculated by using expression (8), allowing, subsequently, n to vary from n_s to n_c in every interval of slip, until crack length achieves the critical failure length. In this matter, the whole da/dN vs crack length is obtained.

Figure 12 shows the model applied to some experimental results obtained by Hobson on a 0.4 C steel. The two limit curves, plotted using equation (1) with n_s upper curve and n_c lower curve, seem to provide reasonable bounds to the experimental crack growth data. Equation (4) derived by Hobson is also plotted in this figure.

Writing equation (6) in terms of n and c and considering that in each interval c is constant (the plastic zone is blocked by a grain boundary) the intergration of equation (6) over each interval gives

$$N_i = \frac{G}{f\Delta\sigma} (\sin^{-1} n_c^1 - \sin^{-1} n_s^1) \qquad (10)$$

and the total life-time is therefore

$$N = \sum_{I=1}^{2a/D} N_1 \quad i = 1, 3, 5 \ldots 2a/D \qquad (11)$$

where D is the grain diameter.

Calculations using this method have been carried out using the data of Hobson to determine lifetime to failure. The results listed in Table II show that the predicted lifetimes are in very good agreement with the experimental results; also given in this table are lifetime predictions obtained by integrating equations (3) and (4) over their respective ranges of applications.

In closing this lecture it seems that the microstructural-sensitive mode of crack growth occurs when the cyclic plastic zone is impeded by an obstacle or barrier. The nature, strength, number and density of these barriers determine not only crack growth rate but also the possibility of crack arrest. Developments or short crack resistant materials can now be accomplished with much more certainty based on the concept of microstructural barriers to crack propagation. Obviously each type of barrier will have its own characteristic arrest period and there will also be an optimum size and distribution of barriers of a given strength for a particular material.

References

Bilby B.A., Cottrell A.H. and Swinden K.H. (1963) proc. R. Soc. Lond. 1272, 304.

Brown M.W. (1986), In The Behaviour of Short Fatigue Cracks, (Ed. K.J. Miller and E.R. de los Rios) MEP London, 423.

Hobson P.D., Brown M.W. and De los Rios E.R. (1986) ibid, 441.

Kitagawa H. and Takahashi S. (1976), 2nd Int. Conf. on the Mechanical Behaviour of Materials (ICM2) Boston, USA, 627.

Liu H.W. and Liu D. (1986), Scripta Metallurgica 16, 595.

Miller K.J. (1986), The Short Crack Problem in Mechanical and Thermal Behaviour of Metallic Materials, Italy 165.

Navarro A. and De los Rios E.R. (1986) Phil Mag. 57, 15; (1988), Fatigue Fract. Engng. Mater. Struct. 11, 383.

Petch N.J. (1953) J. Iron Steel Inst. 174, 25.

Taylor D. (1982) Fatigue Engng. Mater. Struct. 5, 305.

Yoder G.R., Cooley L.A. and Crooker T.W. (1982) Scripta Metallurgica 16, 1021.

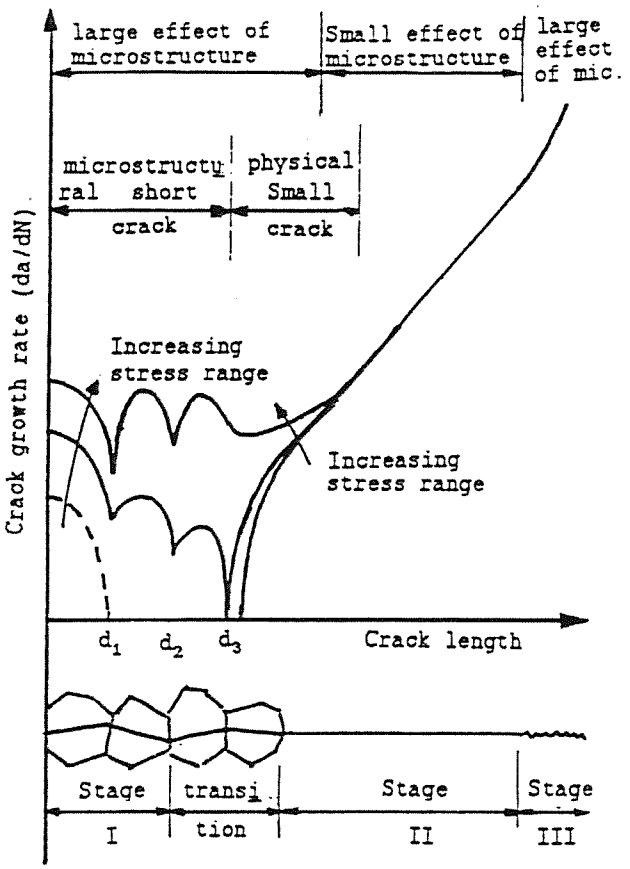

Fig.1 Schematic representation of the various stages in fatigue crack growth.

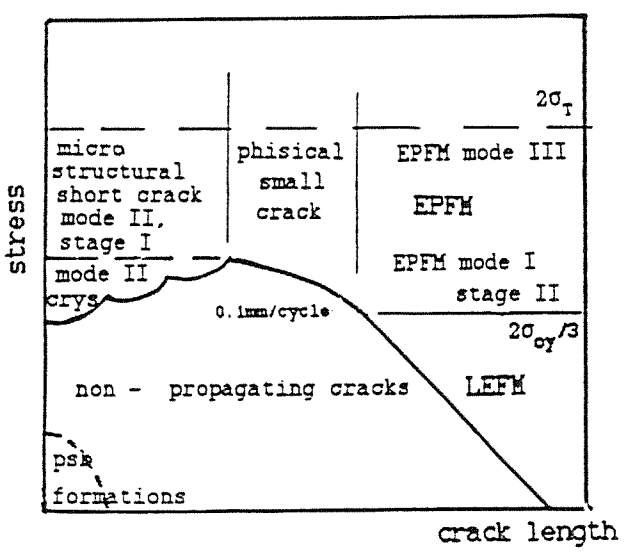

Fig.2 The fatigue mechanisms map of Brown.

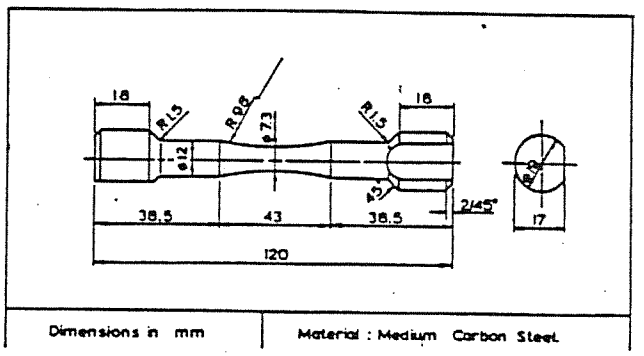

Fig.3 Hour-glass shape specimen.

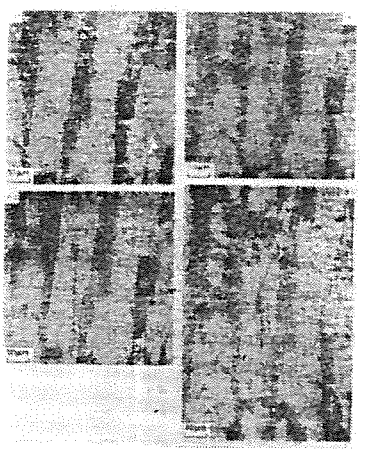

Fig.4 Short crack development in 0.4 C steel. Plastic replica.

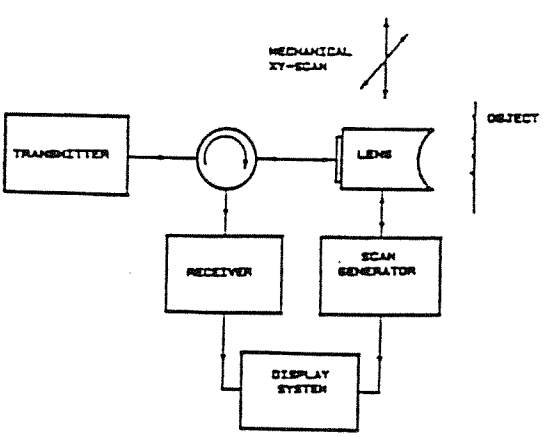

Fig.5 Acoustic microscope block diagram.

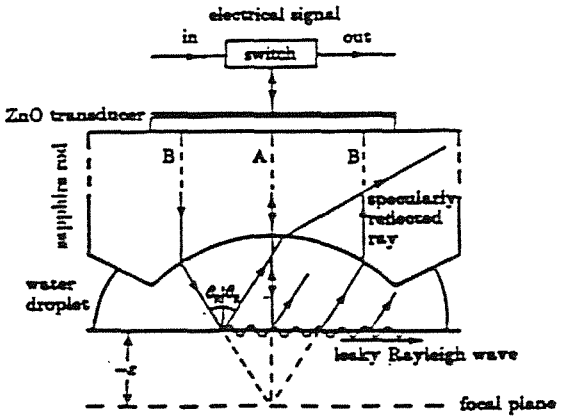

Fig.6 The acoustic lens and main acoustic waves.

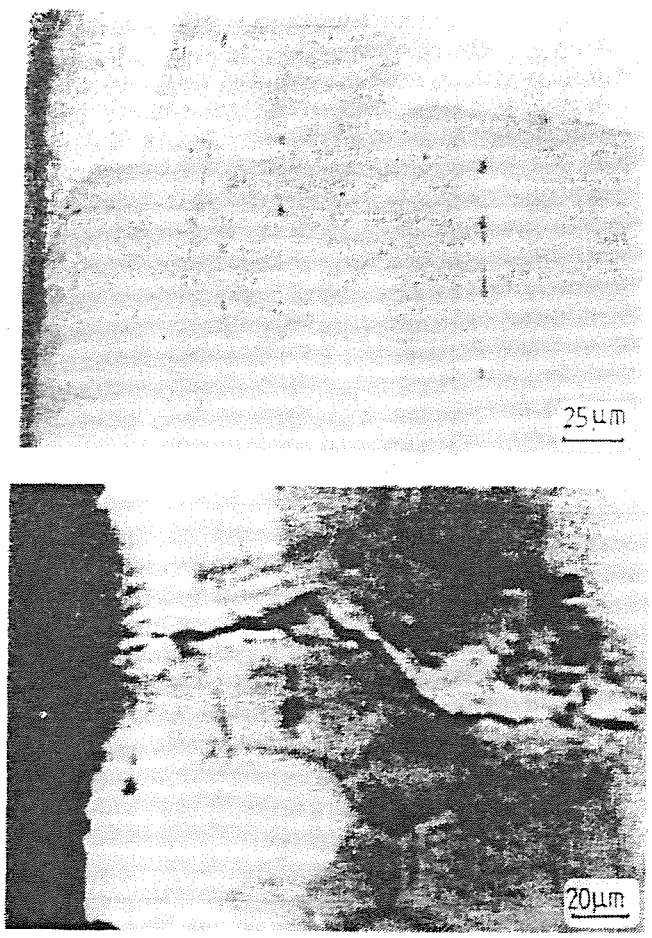

Fig.7 Short crack as detected by
a) Optical microscopy
b) Acoustic microscopy.

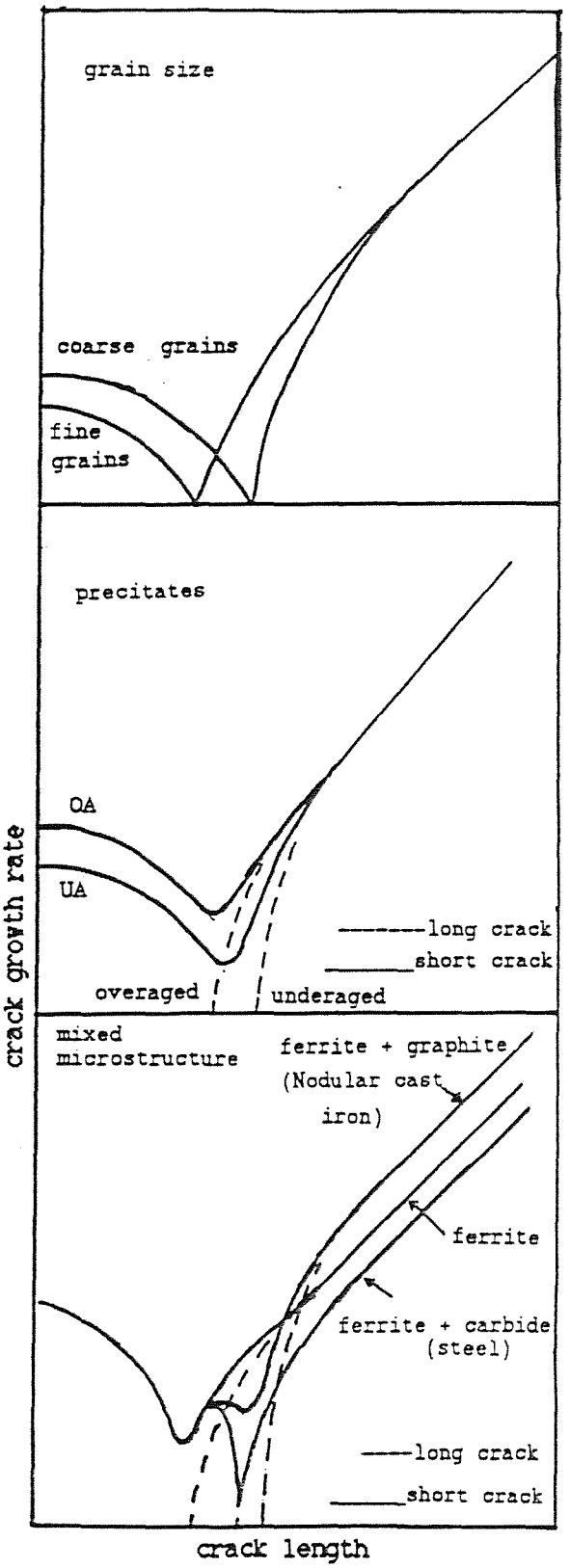

Fig.8 Effect of grain size, precipitation and second phase on fatigue crack growth.

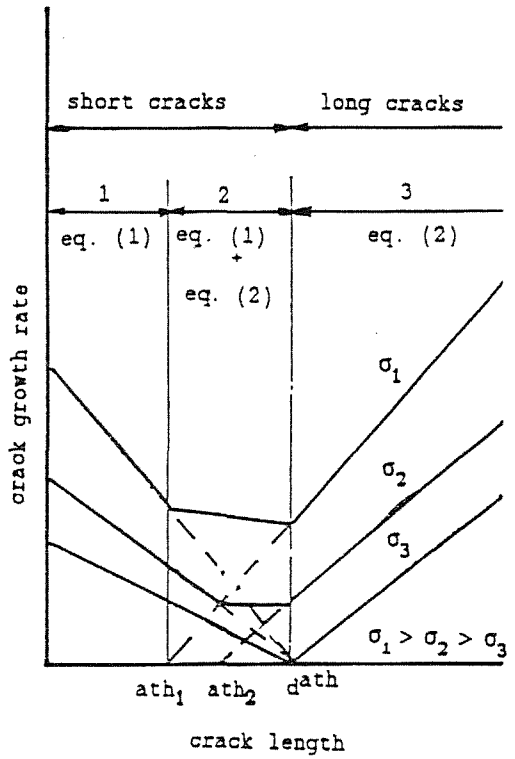

Fig.9 Schematic of low growth rates for short and long fatigue crack growth.

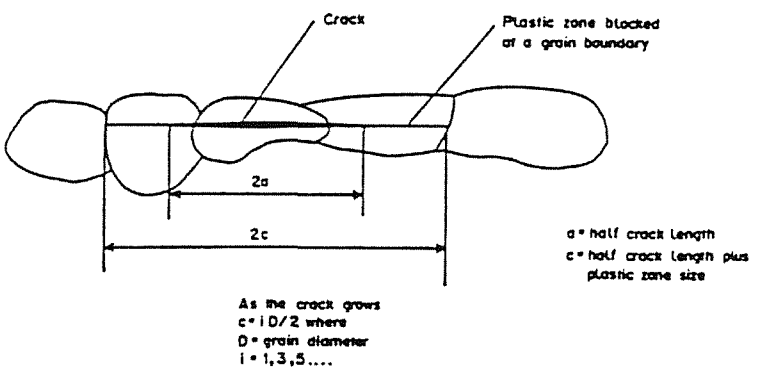

Fig.10 Schematic of a crack and blocked slip band.

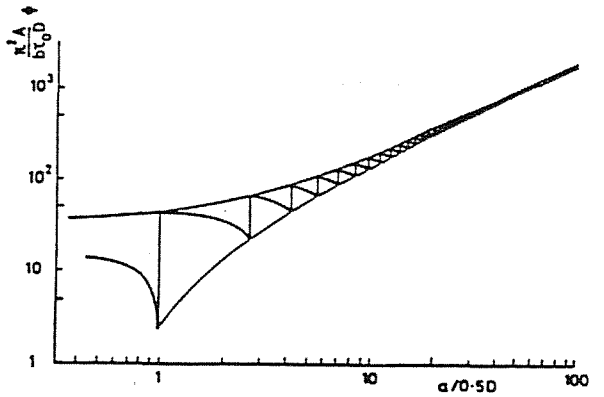

Fig.11 Oscillating pattern of the plastic displacement at the tip of a short crack.

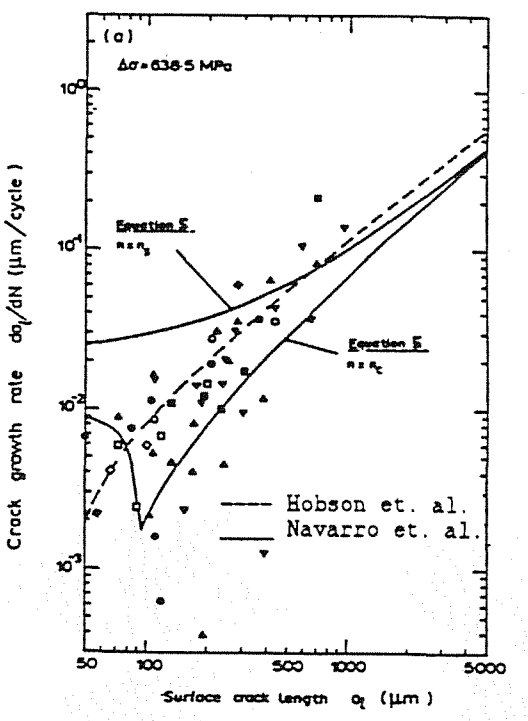

Fig.12 Model predictions and experimental results of crack growth rate in a 0.4 C steel.